

Vibration-Actuated Bistable Micromechanism for Microassembly

D.-A. Wang* and H.-T. Pham**

Institute of Precision Engineering, National Chung Hsing University
250 Kuo Kuang Rd, Taichung, Taiwan, ROC, *daw@nchu.edu.tw
**cslamvien@yahoo.com

ABSTRACT

This paper proposes a novel method to switch an on-substrate bistable micromechanism. An external vibration is exploited to switch the micromechanism between its bistable positions. There is no need to build any actuators on substrate with this method. The vibration-actuated bistable micromechanism (VABM) is vibrated by shaking the entire substrate with a piezo actuator. The vibration provides a simple means of switching the VABM. Finite element analyses are utilized to obtain the nonlinear spring stiffness of the VABM and an analytical model is derived in order to analyze its dynamic behavior. Prototypes of the VABM are fabricated using electroforming. A scenario of the VABM for on-substrate fine positioning of micro components is presented.

Keywords: bistable, micromechanism, vibration

1 INTRODUCTION

Bistable micromechanisms (BMs) are gaining attention in MEMS applications such as memory cells [1], switches [2], relays [3], and valves [4]. One advantage of BMs is that no power is required to keep the mechanism in either of its bistable positions [5]. Most researches utilize on-substrate thermomechanical actuators [6,7] for switching between bistable positions, while others use comb-drive actuators [5,8]. In this investigation, an external vibration is exploited to switch BM between its bistable positions. There is no need to build any on-substrate actuator with this method.

This paper describes a design of a BM actuated by external vibration. The design is based on a BM reported by Wilcox and Howell [6], where their BM is actuated by a thermomechanical actuator. Dissimilar to their actuation method, here, the BM is actuated by shaking the entire substrate with a piezo actuator, requiring no need for built-in driving mechanisms such as thermomechanical or comb-drive actuators. This vibration of the BM via an external vibration source provides a simple means of switching BMs. An analytical model of the vibration-actuated bistable micromechanism (VABM) is derived in order to analyze its dynamic behavior. Prototypes of the VABM are fabricated using an electroforming process. A scenario of the VABM for on-substrate fine positioning of micro components is presented.

2 DESIGN

2.1 Operational principle

A schematic of a VABM investigated here is shown in Fig. 1(a). It consists of flexible folded beams and a shuttle. Fig. 1(b) shows a quarter model of the VABM. A Cartesian coordinate system is also shown in the figure. As the shuttle is moving linearly, besides bending, short and long segments of the folded beam are under tension and compression, respectively. The combined bending, compression and tension in folded beams results in bistable behavior of the device.

The concept of the actuation by external vibration is illustrated in Fig. 2. First, the substrate is shaken at frequency f_1 (see Fig. 2(a)) and this vibration causes the BM to move to its second stable position (see Fig. 2(b)). Next, the substrate is shaken at frequency f_2 (see Fig. 2(c)). This external vibration causes the BM to move to its first stable position.

2.2 Modeling

An equation of motion of a lumped parameter model of the BM shown in Fig. 1(a) is derived to analyze its dynamic behavior. The equation of motion for a simple mass-damper-spring system with excitation $F_{ext}(t)$ from external vibration has the form

$$m\ddot{x} + c\dot{x} + kx = F_{ext}(t) \quad (1)$$

where m , c , and k are the mass, viscous damping coefficient, and spring stiffness of the BM. Assuming Couette air flow between the substrate and the BM, c can be expressed as

$$c = \mu A / d \quad (2)$$

where μ is the viscosity of the fluid in the environment.

A and d are the planar area of the BM and the gap between the substrate and the BM, respectively. The nonlinear spring stiffness, including terms up to ninth order, is written as

$$k = \sum_{i=0}^9 k_i x_i \quad (3)$$

This ninth order stiffness function allows for the detailed modeling of the highly nonlinear force-displacement relation of the BM.

When the BM is actuated by shaking the entire substrate with an external vibration $x = Z \cos(\omega t)$ in the x direction, the inertial force $F_{ext}(t)$ exerted to the BM is

$$F_{ext}(t) = m\omega^2 Z \cos(\omega t) \quad (4)$$

where Z and ω are the amplitude and frequency of the external vibration, respectively.

2.3 Analyses

In order to obtain the nonlinear spring stiffness for a VABM, finite element analyses are carried out. Due to symmetry, only a quarter model is considered. Fig. 1(b) shows a schematic of a quarter model with $L_1 = 300 \mu\text{m}$, $L_0 = 900 \mu\text{m}$, $L_s = 200 \mu\text{m}$, $t_1 = 5 \mu\text{m}$, $t_0 = 40 \mu\text{m}$, $t_s = 9 \mu\text{m}$, and $\theta = 2.3^\circ$. The thickness t of the device is $5 \mu\text{m}$. In the analyses, the material of the device is assumed to be linear elastic and isotropic. The Young's modulus E is taken as 207 GPa, and the Poisson's ratio ν is taken as 0.31. The commercial finite element program ABAQUS is employed to perform the computations.

A force-displacement curve and a potential energy curve of the VABM are shown in Fig. 3(a) and 3(b), respectively. We selected a ninth order function, Eq. (3), to fit the simulation data in Fig. 3(a). The values of the coefficients of Eq. (3) are listed in Table 1. The two local minimums of the energy curve correspond to the two stable positions of the VABM.

In order to simulate the dynamic behaviors of the VABMs, Park method [11] is used to solve the governing nonlinear differential equations, Eqs. (1)-(4). Fig. 4 shows time responses of the VABM vibrated at different frequencies and amplitudes. As shown in Fig. 4(a), when the external vibration with $\omega/2\pi = 5.1 \text{ kHz}$ and $Z = 1 \mu\text{m}$ is applied to the substrate, the VABM is switched from stable position 1 to stable position 2. When the substrate is vibrated at $\omega/2\pi = 3.96 \text{ kHz}$ and $Z = 2 \mu\text{m}$, the VABM is found to switch from stable position 2 to stable position 1.

3 FABRICATION AND TESTING

VABMs have been fabricated by a simple electroforming process on glass substrates. Fig. 5 shows the fabrication steps, where only two masks are used. First, a $2 \mu\text{m}$ -thick titanium seed layer is sputter-coated on the whole glass substrate. Next, a $5 \mu\text{m}$ -thick photoresist (AZ4620) is coated and patterned to prepare a mold for electrodeposition of a copper sacrificial layer. Following that, a $5 \mu\text{m}$ -thick photoresist (AZ4620) is coated and patterned on top of the copper sacrificial layer. Into this

mold, a $5 \mu\text{m}$ -thick nickel layer is electrodeposited using a low-stress nickel sulfamate bath with the chemical compositions listed in Table 2. Finally, the photoresist and copper sacrificial layers are removed to release the nickel microstructures.

Fig. 6 shows an OM photo of a fabricated device. The fabricated devices will be tested using the experimental apparatus shown in Fig. 7. A piezo actuator (PPA20M, Cedrat Technologies) is used to shake the substrate. Further experimental work is underway.

4 A VABM FOR MICROASSEMBLY

A scenario of the VABM for on-substrate fine positioning of micro components is presented. The device shown in Fig. 8(a) includes a clamp and two actuating BMs. It is fabricated on a glass substrate. Fig. 8 illustrates a four-step operation of the device. First, the substrate is shaken at the frequency f_1 , and this vibration resonates only BM 1 (see Fig. 8(a)), causing BM 1 to move towards its second stable position (see Fig. 8(b)). This motion causes the clamp to push a micro component against an anchored fixture, achieving precise positioning (see Fig. 8(b)). Next, the substrate is shaken at the frequency f_2 . This external vibration resonates only BM 2 (see Fig. 8(c)), causing BM 2 to move towards its second stable position. This motion causes the clamp to return to its original position (see Fig. 8(d)), releasing the positioned component.

The force required to move the clamp between its stable positions, R_c , is designed to be smaller than the forces for the BM 1 and BM 2, R_1 and R_2 , respectively (see Fig. 9). The subscripts f and b in Fig. 9 represent the forward (from stable position 1 to stable position 2) and backward (from stable position 2 to stable position 1) motion, respectively. For assembly of the micro component, R_{1f} must be greater than the sum of R_{2b} and R_{cf} . For release of the micro component, R_{2f} must be greater than the sum of R_{1b} and R_{cb} . It is also designed that the clamp has a different natural frequency from those of BM 1 and BM 2. Since the dimensions for BM 1 and BM 2 are the same except their shuttle masses, their force-displacement curves are the same as shown in Fig. 9. However, with different shuttle masses, BM 1 and BM 2 have different natural frequencies. Finite element analyses are carried out to obtain the nonlinear spring constants of the BMs. Based on numerical simulations, frequencies and amplitudes for BM 1 and BM 2 are found to move the clamp between its stable positions. Further experimental work is underway.

5 CONCLUSIONS

External vibration is proposed to switch a BM between its stable positions. The frequencies and amplitudes for the dynamic switching are found by solving the nonlinear equation of motion of the BM. The selective vibration provides a simple means of switching the BM. For demonstration of the effectiveness of the BM for

microassembly, prototypes of BMs, a clamp, and micro components are fabricated on glass substrates using electroforming. A scenario of the BM for on-substrate fine positioning of micro components is presented.

REFERENCES

- [1] B. Hälg, "On a nonvolatile memory cell based on micro-electro-mechanics," in Proc. IEEE MEMS 1990 Conference, pp. 172-176.
- [2] M. Freudenreich, U.M. Mescheder, G. Somogyi, "Design considerations and realization of a novel micromechanical bi-stable switch," in Transducers 2003 Workshop, pp. 1096-1099.
- [3] T. Gomm, L.L. Howell and R.H. Selfridge, "In-plane linear displacement bistable microrelay," J. Micromech. Microeng. 12, 257-264, 2002.
- [4] B.Wagner, H.J. Quenzer, S. Hoerschelmann, T. Lisee and M. Jueress, "Bistable microvalve with pneumatically coupled membranes," in Proc. IEEE MEMS 1996 Conference, pp. 384-388.
- [5] J. Casals-Terre and J. Shkel, "Snap-action bistable micromechanism actuated by nonlinear resonance," in IEEE Sensors 2005, pp. 893-896.
- [6] D.L. Wilcox and L.L. Howell, "Fully compliant tensural bistable micromechanisms (FTBM)," J. Microelectromech. Syst., 14, 1223-1235, 2005.
- [7] J. Qiu, J.H. Lang and A.H. Slocum, "A curved-beam bistable mechanism," J. Microelectromech. Syst., 14, 1099-1109, 2005.
- [8] K.B. Lee, A.P. Pisano and L. Lin, "Nonlinear behaviors of a comb drive actuator under electrically induced tensile and compressive stresses," J. Micromech. Microeng., 17, 557-566, 2007.
- [9] W.Y. Tseng and J. Dugundji, "Nonlinear vibrations of a buckled beam under harmonic excitation," J. Applied Mechanics, 38, 467-476, 1971.
- [10] N. Yamaki and A. Mori, "Non-linear vibrations of a clamped beam with initial deflection and initial axial displacement. I - Theory," Journal of Sound and Vibration, 71, 333-346, 1980.
- [11] A.F. D'Souza and V.K. Garg, "Advanced Dynamics: Modeling and Analysis," Prentice-Hall, 1984.

k_0	-9.945×10^{-15}
k_1	6.286×10^{-12}
k_2	-1.678×10^{-9}
k_3	2.445×10^{-7}
k_4	-2.083×10^{-5}
k_5	0.001016
k_6	-0.02369
k_7	-0.001379
k_8	7.784
k_9	0.3754

Table 1: Values of the coefficients of the nonlinear spring stiffness function.

Chemical/Plating Parameter	Amount/Value
Nickel sulfamate ($\text{Ni}(\text{NH}_2\text{SO}_3)_2 \cdot 4\text{H}_2\text{O}$)	450 g/L
Boric acid (H_3BO_3)	35 g/L
Nickel chloride ($\text{NiCl}_2 \cdot 6\text{H}_2\text{O}$)	4 g/L
Stress reducer	17 ml/L
Leveling agent	17 ml/L
Wetting agent	2 ml/L
Bath temperature	45 °C
Plating current type	dc current
pH of the solution	4
Plating current density	0.113 A/dm ²
Deposition rate	0.071 $\mu\text{m}/\text{min}$
Anode-cathode spacing	100 mm
Anode type	titanium

Table 2: Chemical composition and operation conditions for the low-stress nickel electroplating solution.

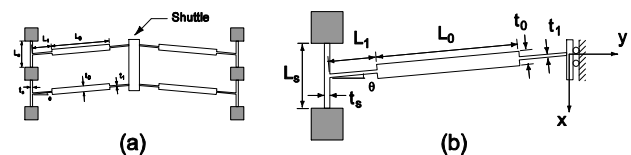


Figure 1: Schematics of a VABM. (a) A full model. (b) A quarter model.

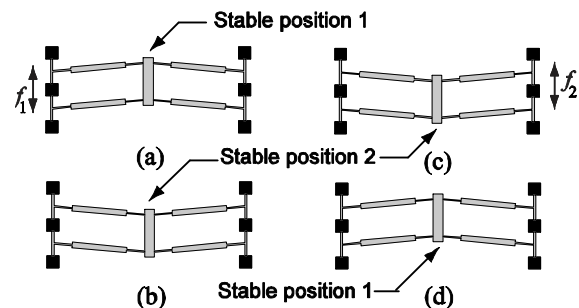


Figure 2: Actuation by external vibration.

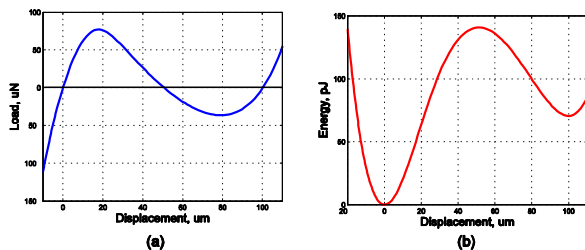


Figure 3: (a) A force-displacement curve and (b) an energy curve of a VABM.

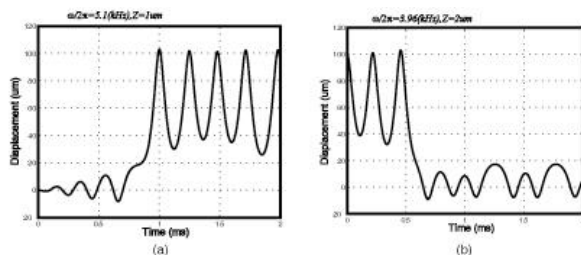


Figure 4: Simulated displacement with respect to time: (a) switching from stable position 1 to stable position 2 and (b) switching from stable position 2 to stable position 1.

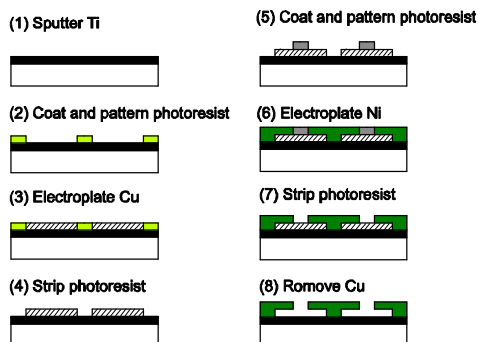


Figure 5: An electroforming process.

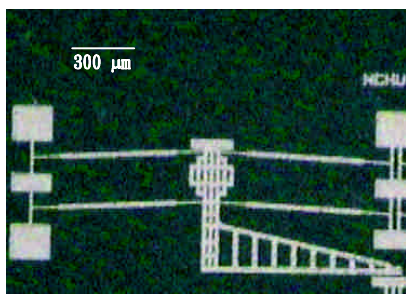


Figure 6: An optical micrograph of a VABM.

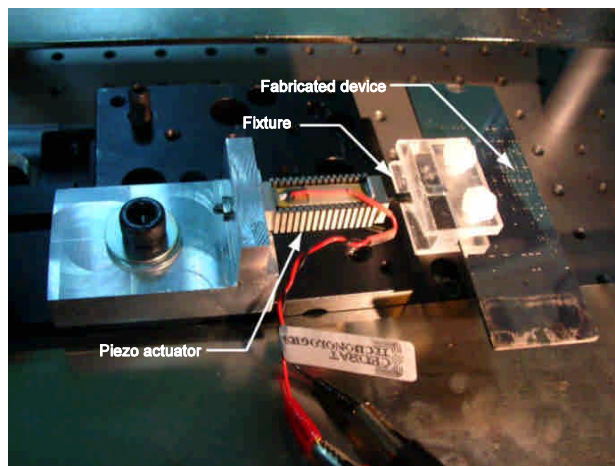


Figure 7: Experimental apparatus.

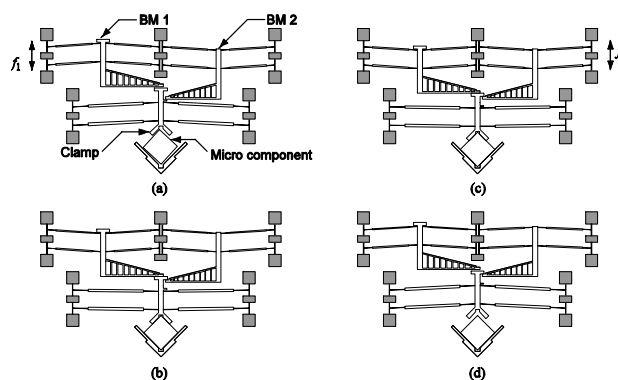


Figure 8: A scenario of a VABM for on-substrate fine positioning of micro components.

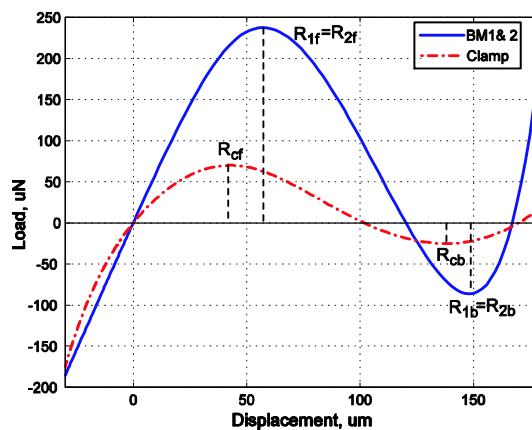


Figure 9: Force-displacement curves of BM 1, BM 2 and the clamp.